

ANPrompt: Anti-noise Prompt Tuning for Vision-Language Models

Yansheng Gao^{1,3}, Yufei Zheng^{2,3}, Jinghan Qu^{2,3}, Zixi Zhu^{2,3}, Yukuan Zhang^{1,3}, Shengsheng Wang^{1,2,3,*}

¹College of Computer Science and Technology, Jilin University

²College of Software, Jilin University

³Key Laboratory of Symbolic Computation and Knowledge Engineering of Ministry of Education, Jilin University

Abstract

Prompt tuning has emerged as an efficient and effective technique for adapting vision-language models (VLMs) with low computational overhead. However, existing methods often overlook the vulnerability of prompt-tuned VLMs to weak semantic perturbations—such as subtle image or text noise—that degrade their generalization to unseen classes. To address this limitation, we propose ANPrompt, a novel prompt tuning framework designed to enhance robustness under such perturbations. ANPrompt first constructs weak noise text features by fusing original and noise-perturbed text embeddings, which are then clustered to form noise prompts. These noise prompts are integrated with learnable prompt tokens to generate anti-noise prompts, which are injected into the deeper layers of both image and text encoders. To further capture the noise-aware visual semantics, ANPrompt computes the Noise-Resistant Visual Prompt Prototype (NRVPP) by averaging the output prompt tokens from the vision encoder. Finally, ANPrompt introduces alignment, robustness, and anti-noise objectives by computing a Weak semantic noise Alignment Loss (WALoss) alongside the standard cross-entropy and sim loss. Experiments across 11 benchmarks demonstrate that ANPrompt consistently outperforms existing prompt tuning approaches, achieving superior robustness to semantic noise and improved generalization to novel categories.

Introduction

Vision-language models (VLMs) like CLIP have demonstrated impressive performance on open-vocabulary recognition tasks (Hua et al. 2025; Weng et al. 2023; Xu et al. 2024), but adapting such large models to downstream tasks via full fine-tuning can be computationally prohibitive. To address this, prompt tuning (Zhu et al. 2024; Lafon et al. 2024; Shi et al. 2024) has emerged as a lightweight alternative by optimizing only a small set of learnable tokens, achieving state-of-the-art results across various domains. Despite its efficiency, early prompt tuning methods such as CoOp (Zhou et al. 2022b) often overfit to seen classes, resulting in limited generalization to novel categories and vulnerability to subtle semantic perturbations.

To enhance transferability, recent approaches have integrated inductive biases into the prompting process. For in-

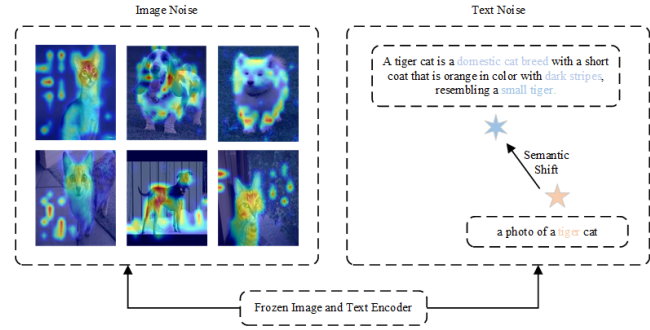


Figure 1: Weak semantic perturbations in image and text: CAMs may highlight irrelevant regions (e.g., background or co-occurring objects), while subtle textual cues (e.g., “dark stripes”) may mislead class semantics (e.g., shift from “cat” to “tiger”).

stance, CoCoOp conditions prompts on image features to mitigate overfitting; KgCoOp constrains semantic drift by leveraging frozen text embeddings; and MaPLe adopts multimodal prompts to achieve more robust alignment. More advanced techniques such as PromptSRC and CoPrompt regularize prompt learning using frozen zero-shot logits, while MMRL and TAC construct shared or clustered semantic spaces. Although designed to reduce overfitting, consistency constraints based on frozen features may introduce noise information such as misleading text or visual clutter caused by domain gaps, ultimately weakening the robustness of Vision-Language Models.

As shown in Figure 1, we define subtle noise in images and texts as weak semantic perturbations, which appear as either misleading text (e.g., “a cat resembling a small tiger”) or visual noise (e.g., background clutter or co-occurring objects). While high-quality image-text pairs exhibit clear object focus and accurate descriptions, existing prompt tuning methods often struggle to handle such subtle shifts, leading to significant performance drops when adapting to novel categories. This highlights the urgent need for VLMs capable of learning robust, noise-resilient cross-modal representations to maintain alignment consistency and improve generalization.

To address the issue of weak semantic perturbations, we

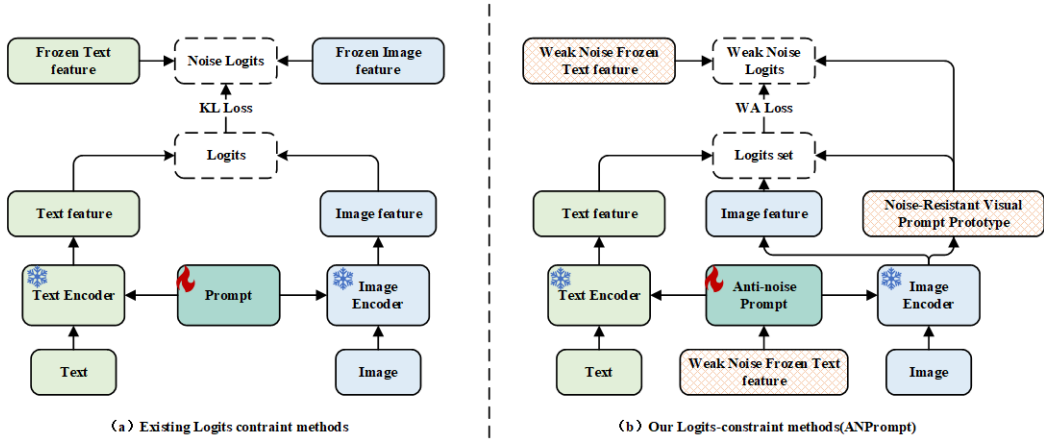


Figure 2: Different with existing methods use frozen logits as constraint, risking overfitting under weak semantic perturbations. ANPrompt introduces weak semantic perturbations to generate soft logits and anti-prompt to improves generalization.

propose **ANPrompt** — a prompt tuning framework specifically designed to enhance robustness under such perturbations. As illustrated in Figure 2, existing methods rely on frozen feature constraints and thus tend to suffer from overfitting when exposed to weak semantic perturbations. In contrast, our ANPrompt framework intentionally incorporates weak semantic perturbation information into prompt tokens and logits, thereby boosting the robustness of both the learned prompts and class distributions in scenarios involving weak semantic perturbations. Specifically, ANPrompt randomly samples two intra-class descriptions from a language cache: a *main text* that conveys core semantics, and a *noise text* that introduces minor linguistic variations. Their fusion generates a *Weak Noise Frozen Text Feature*, which incorporates weak semantic perturbation information while preserving class identity. These features are clustered into *noise prompts* and injected as biases into learnable tokens, forming *Anti-noise Prompts*. These prompts are then inserted into the higher layers of both text and vision encoders to introduce weak semantic perturbation information at the prompt representation level. After encoding, ANPrompt extracts image Feature, text Feature, and the **Noise-Resistant Visual Prompt Prototype (NRVPP)**. The latter is obtained by mean-pooling the visual prompt tokens from the final layer of the visual encoder. Since Anti-noise Prompts are injected into deeper encoder layers, the resulting NRVPP inherit weak semantic perturbations.

To stabilize training under both weak semantic perturbations, we introduce a KL divergence-based *Weak Alignment Loss (WALoss)* between Weak Noise Logits and Logits set, which enforces alignment consistency under controlled weak semantic perturbations. Additionally, we employ a CE and sim loss to enable the model to learn task-relevant knowledge under weak semantic perturbations. By combining these losses, ANPrompt can improve the robustness of VLMs under weak semantic perturbations.

Extensive experiments conducted on 11 benchmarks and base-to-new splits show that ANPrompt significantly outperforms existing prompt tuning methods, achieving state-of-

the-art performance in terms of robustness and generalization.

Our main contributions are summarized as follows:

- We propose **ANPrompt**, a prompt tuning framework that improve the robustness of VLMs by injecting weak semantic perturbations into both prompt tokens and logits pathways.
- We introduce a **Weak semantic noise Alignment Loss (WALoss)** to enforce alignment consistency under controlled weak semantic perturbations.
- We develop a **weak semantic perturbations prompt injection mechanism** that clusters weak noise frozen text features into noise prompts and injects them into learnable tokens to get anti-noise prompt, which is used to inject weak semantic perturbations at the prompt representation level.
- ANPrompt achieves state-of-the-art performance on 11 benchmark datasets under base-to-new generalization settings.

Related Work

Vision-Language Models

Pretrained vision-language models (VLMs) such as CLIP (Radford et al. 2021) and ALIGN (Jia et al. 2021) achieve strong open-vocabulary and cross-modal capabilities through contrastive learning on large-scale image-text pairs. Building on this foundation, models like BLIP (Li et al. 2022), FILIP (Yao et al. 2021), Florence (Yuan et al. 2021), and LiT (Zhai et al. 2022) enhance fine-grained alignment and data efficiency via retrieval augmentation(Li et al. 2024a), self-supervised learning, and stronger backbones. NLIP (Huang et al. 2023) further improves robustness by introducing noise-harmonization based on alignment uncertainty and noise-completion via concept-guided caption generation. These advances enable effective zero-shot and few-shot transfer for tasks such as retrieval, classification, and grounding. However, adapting such large

models to downstream tasks (Li et al. 2025a, 2023) remains costly due to domain shifts and the high overhead of full fine-tuning. To address this, parameter-efficient tuning methods—such as adapter-based approaches (Gao et al. 2024; Yang et al. 2024b; Song et al. 2023) and prompt learning (Zhou et al. 2022b,a; Khattak et al. 2024)—have been proposed to enable lightweight adaptation without retraining the entire model.

Prompt Learning

Prompt learning has become an efficient strategy to adapt VLMs without full fine-tuning. Early methods such as CoOp (Zhou et al. 2022b) and CoCoOp (Zhou et al. 2022a) explore soft and image-conditioned prompts to enhance generalization. Subsequent works improve robustness and transferability through multimodal regularization (MaPLe (Khattak et al. 2023a), PromptSRC (Khattak et al. 2023b)), gradient alignment (ProGrad (Zhu et al. 2023)), hierarchical and knowledge-guided prompts (HPT (Wang et al. 2024), TCP (Yao, Zhang, and Xu 2024)), and distillation-based initialization (CLIP-kd (Yang et al. 2024a), ComKD-CLIP (Chen et al. 2024), PromptKD (Li et al. 2024b), CasPL (Wu et al. 2024)). Other methods focus on attribution-based prompting (ATPrompt (Li et al. 2024c)), two-stage decoupled optimization (DPC (Li et al. 2025b), DePT (Zhang et al. 2024), 2SFS (Farina et al. 2025)), or cross-modal adapters (MMA (Yang et al. 2024b)) for few-shot settings. Consistency learning (CoPrompt (Roy and Etemad 2024)) and task-aware clustering (TAC (Hao et al. 2025)) further enhance adaptability. However, these approaches largely target generalization and efficiency, with limited attention to robustness against weak semantic perturbations.

Prompting under Weak Semantic Perturbation Noise

Recent works have explored robust prompt learning under noisy conditions. Methods such as NLPrompt (Pan et al. 2025), JoAPR (Guo and Gu 2024), and ArGue (Tian et al. 2024) mitigate label noise through loss design, sample filtering, and LLM-generated attributes, while Clip-Cleaner (Feng, Tzimiropoulos, and Patras 2024) leverages CLIP-based sample selection to decouple training from noise filtering. However, these approaches mainly focus on filtering noise, which risks discarding informative variations and often limits generalization. In contrast, we propose ANPrompt, which embraces weak semantic perturbations as supervision signals. By integrating perturbed prompts with clustering-based bias representations, ANPrompt enables robust and discriminative prompt learning without relying on brittle filtering heuristics.

Methodology

Preliminary

Vision-language models (VLMs) such as CLIP (Radford et al. 2021) learn a joint embedding space for images and texts through contrastive learning over large-scale image-text pairs. These models exhibit strong zero-shot generaliza-

tion but are highly sensitive to semantic variations in either modality.

A typical VLM consists of a vision encoder and a text encoder. The vision encoder tokenizes the input image into patches, encodes them through Transformer layers, and outputs a class token representing global semantics. The text encoder processes class-dependent prompts (e.g., “a photo of a [CLASS]”), encodes them with Transformers, and uses the [EOS] token as the prompt embedding.

The classification score for class c is computed via cosine similarity:

$$p(y = c | f) = \frac{\exp(\text{sim}(f, w_c)/\tau)}{\sum_{i=1}^C \exp(\text{sim}(f, w_i)/\tau)} \quad (1)$$

where f is the image feature, w_c is the text feature for class c , τ is a learnable temperature, and $\text{sim}(\cdot)$ denotes cosine similarity.

Overview

We propose **ANPrompt** — a robust prompt tuning framework that injects *weak semantic perturbations* into the prompting and alignment processes to enhance the robustness of VLMs under such perturbations. Specifically, ANPrompt simulates weak semantic perturbations by fusing two intra-class textual descriptions from the language cache, generating a *Weak Noise Frozen Text Feature*. These Weak Noise Frozen Text Features are clustered to obtain noise prompts, which are then projected and added to learnable prompt tokens to form *Anti-noise Prompts*. These prompts are inserted into the deeper layers of both vision and text encoders, enabling ANPrompt to inject weak semantic perturbations at the prompt level. Subsequently, prompted image features, prompted text features, and NRVPP can be obtained for computing alignment logits, robustness logits, weak noise logits, and anti-noise logits. During training, ANPrompt combines the Weak Semantic Noise Alignment Loss (WALoss), cross-entropy loss, and SimLoss to enhance the robustness of VLMs under weak semantic perturbations.

ANPrompt Framework

As shown in Figure 3. The ANPrompt framework proceeds through four sequential stages: (1) Weak Noise Frozen Text Feature Construction, (2) Anti-noise Prompt Generation, (3) Feature Encoding, and (4) Logit Computation.

1. Weak Noise Frozen Text Feature Generation: ANPrompt samples two intra-class descriptions: a *main text* that encodes core semantics, and a *noise text* that introduces subtle phrasing variations (e.g., attribute reordering). These two texts are encoded by the frozen CLIP text encoder into f_m and f_n respectively, and fused as follows:

$$f_w = f_m + \alpha f_n \quad (2)$$

where α regulates the perturbation strength. Since the *Weak Noise Frozen Text Feature* f_w incorporates contextual information from different sentences, it inevitably captures contextual cues that lean toward semantically adjacent yet incorrect classes. Consequently, weak noise text features inherently encode weak semantic perturbations information.

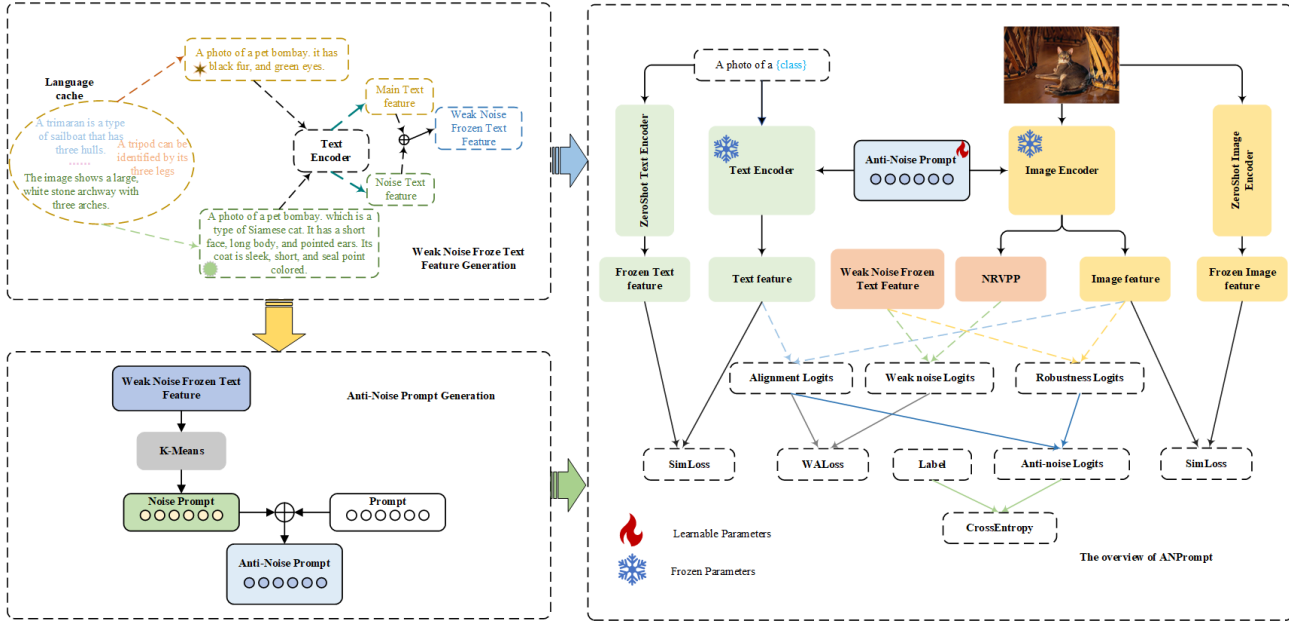


Figure 3: ANPrompt randomly samples a main and a noise sentence from the same class to construct the Weak Noise Frozen Text Feature, which is used to generate Anti-noise Prompts. These prompts are injected into the encoder’s deep layers. During encoding, we extract the Prompted Image/Text Features and the Noise-Resistant Visual Prompt Prototype (NRVPP) to compute four types of logits, which are supervised by WALoss and auxiliary losses to improve robustness against weak semantic perturbations.

2. Anti-noise Prompt Generation: To map weak semantic perturbation information into the prompt space, ANPrompt performs K-means clustering on all f_w to extract representative semantic centers, which are referred to as *noise prompts*. These noise prompts are added to the learnable prompt tokens P_c to form intermediate anti-noise prompts P_a . These intermediate prompts are then fed into two separate fully connected layers to generate modality-specific Anti-noise Prompts, which is injected into the deeper layers of both encoders.

3. Feature Encoding. After prompt injection, we extract three types of features: the **Prompted Image Feature** f_v , encoded from the final image class token; the **Prompted Text Feature** f_t , derived from the final [EOS] token; and the **Noise-Resistant Visual Prompt Prototype (NRVPP)** f_N , obtained by mean-pooling the visual Anti-noise Prompts after encoding, which captures weak semantic perturbations information.

4. Logit Computation. We compute four sets of logits: the **Alignment Logits** $\ell_A = f_v \cdot f_t^\top$, which measure the similarity between the prompted image and text features; the **Robustness Logits** $\ell_R = f_v \cdot f_w^\top$, which assess the model’s robustness against weak semantic noise in text; the **Weak Noise Logits** $\ell_W = f_N \cdot f_w^\top$, which reflect the alignment between noise-resistant visual features and weakly perturbed text features; and the **Anti-noise Logits** $\ell_{\text{final}} = \theta \ell_A + (1 - \theta) \ell_R$, which integrate alignment and robustness for final prediction.

To stabilize training under weak semantic perturbations, we apply \mathcal{L}_{WA} between ℓ_W and ℓ_A for alignment consistency

under weak semantic perturbations, \mathcal{L}_{CE} on ℓ_{final} for task supervision, and \mathcal{L}_{sim} between frozen and prompted features to enhance semantic consistency.

The final loss is:

$$\mathcal{L} = \mathcal{L}_{\text{CE}} + \lambda \mathcal{L}_{\text{sim}} + \gamma \mathcal{L}_{\text{WA}} \quad (3)$$

where \mathcal{L}_{CE} denotes a cross-entropy loss, \mathcal{L}_{sim} represents a cosine loss, and \mathcal{L}_{WA} is defined as follows. λ serves as the weight of \mathcal{L}_{sim} , while γ is a variance-adaptive weight used to regulate the strength of weak semantic perturbations.

Weak Noise Alignment Loss

To enforce alignment consistency under weak semantic perturbations, we introduce a KL divergence-based *Weak Alignment Loss* (\mathcal{L}_{WA}) that minimizes the divergence between ℓ_W and ℓ_A . Since KL divergence measures the discrepancy between distributions, minimizing it encourages the perturbed prediction ℓ_W to stay close to the original alignment ℓ_A , penalizing semantic shifts and improving robustness while preserving alignment structure.

To compute \mathcal{L}_{WA} , we first derive ℓ_A from the prompted image and text features. Then, to obtain ℓ_W , we compute the noise-resistant visual prototype f_N by averaging the visual prompt token features $f_v^o \in \mathbb{R}^{N \times C}$:

$$f_N = \frac{1}{N} \sum_{i=1}^N f_v^o(i) \quad (4)$$

This averaging suppresses token-level variations and mitigates *visual semantic distraction*, especially under anti-prompts with weak semantic noise, where individual tokens

may attend to irrelevant regions such as backgrounds or co-occurring objects. The weak noise logits are then computed as:

$$\ell_W = f_N \cdot f_w^\top \quad (5)$$

Finally, the weak alignment loss is defined as:

$$\mathcal{L}_{WA} = \gamma \cdot \text{KL}(\text{softmax}(\ell_R) \parallel \text{softmax}(\ell_W)) \quad (6)$$

with the variance-adaptive weight γ given by:

$$\gamma = \frac{1}{\text{std}(\ell_R) \cdot |\ell_R| + \epsilon_0} \quad (7)$$

where $\text{std}(\ell_R)$ denotes the standard deviation over all elements in ℓ_R , $|\ell_R|$ represents the total number of elements (i.e., `numel()` of logits), and ϵ_0 is a small constant to prevent division by zero. This global scaling dynamically adjusts the loss weight based on the dispersion and size of the logits, stabilizing optimization under varied prediction confidence levels.

Weak Semantic Perturbations Prompt Injection Mechanism

We introduce a prompt injection mechanism based on weak semantic perturbations. Specifically, we first cluster the weak noise frozen text features $f_w \in \mathbb{R}^{N \times C}$ into K noise prompts $P_w \in \mathbb{R}^{k \times C}$ using K-Means, where k matches the number of learnable prompt tokens $P_c \in \mathbb{R}^{k \times C}$ to ensure one-to-one integration.

These noise prompts are added to the learnable tokens to form the anti-noise prompt:

$$P_a = P_c + \epsilon P_w \quad (8)$$

where ϵ controls the strength of injected weak perturbations. The anti-noise prompt P_a is then projected into modality-specific spaces via a mapping layer.

Finally, the projected prompts P_a^{image} and P_a^{text} are injected into the visual and textual input sequences:

$$\{P_a^{\text{image}}, e_{\text{cls}}, e_1, e_2, \dots, e_M\} \quad (9)$$

$$\{t_{\text{SOS}}, P_a^{\text{text}}, t_1, t_2, \dots, t_L, c_k, t_{\text{EOS}}\} \quad (10)$$

This injection enriches the prompt space with weakly perturbed semantic cues, promoting robustness against subtle noise while maintaining structural alignment with the original prompt format.

Experiments

Evaluation Task

Base-to-Novel Generalization To assess the zero-shot generalization capability of ANprompt, we divide each dataset into base and novel categories. The model is trained on the base categories using a few-shot setting, and its performance is evaluated on both the base and novel categories without additional training.

Cross-Dataset Evaluation To examine the transferability of the model across datasets, we conduct experiments where the model is trained on a few-shot subset of the ImageNet dataset and directly evaluated on other datasets, without any further adaptation or fine-tuning.

Domain Generalization To test the model’s resilience to domain shift, we use the ImageNet-trained model and evaluate it on four distinct ImageNet-derived datasets that introduce various domain differences, allowing us to measure performance under out-of-distribution scenarios.

Evaluation Settings

Datasets In the tasks of Base-to-New Generalization and Cross-Dataset Evaluation, we followed the experimental setup of CoOp (Zhou et al. 2022b), and evaluated on 11 public datasets, including ImageNet, Caltech (Fei-Fei, Fergus, and Perona 2004), OxfordPets (Parkhi et al. 2012), Flowers (Nilsback and Zisserman 2008), Food101 (Bossard, Guillaumin, and Gool 2014), StanfordCars (Krause et al. 2013), FGVCAircraft (Maji et al. 2013), EuroSAT (Helber et al. 2019), UCF101 (Kay et al. 2017), DTD (Cimpoi et al. 2014) and SUN397 (Xiao et al. 2010). We also use ImageNet (Deng et al. 2009) as the source dataset, and use its four variants ImageNetV2 (Recht et al. 2019), ImageNet-Sketch (Wang et al. 2019), ImageNet-A (Hendrycks et al. 2021b) and ImageNet-R (Hendrycks et al. 2021a) as the target dataset to evaluate the domain generalization task.

Implementation Details We set the learning rate to 0.001 and adopt the Adam optimizer to train ANPrompt. The model is trained for 10 epochs with a batch size of 4, using ViT-B/16 as the vision backbone. For the LLM cache, we incorporate prompts from CoPrompt (Roy and Etemad 2024) and HPT (Wang et al. 2024). And we set the θ and α with 0.7 and 0.001. All experiments are conducted on a single NVIDIA RTX 3090 Ti GPU. Reported results are averaged over three random seeds.

Experimental Performance

We compare the results of our method on three evaluation tasks with other advanced prompt learning methods, including zero-shot CLIP and some prompt learning methods, such as CoOp (Zhou et al. 2022b), CoCoOp (Zhou et al. 2022a), MaPLe (Khattak et al. 2023a), PromptSRC (Khattak et al. 2023b), CoPrompt (Roy and Etemad 2024), TextRefiner (Xie et al. 2025) and MMRL (Guo and Gu 2025). We also added some targeted ablation experiments to prove the effectiveness of the proposed ANPrompt method.

Base-to-New Generalization Table 1 shows the performance of ANPrompt and other comparison methods on B2N generalization tasks. Compared with the most advanced MMRL method, ANPrompt improves the base class by 0.44% and the new class by 0.43%. Combining the base class and the new class, ANPrompt achieves a performance improvement of 0.44% on the harmonic average. It is worth noting that compared with MMRL (Guo and Gu 2025), ANPrompt achieves significant performance improvement on EuroSAT dataset: 6.03% on new class and 3.31% on harmonic average. By transforming weak semantic noise into constructive training signals, ANPrompt achieves performance improvement by fusing complementary semantic perturbation sentences.

Table 1: Comparison with state-of-the-art methods on base-to-novel generalization. The best accuracies are bold. We can see that our method achieves the best performance compared with other state-of-the-art methods.

Method	Ref.	Average			ImageNet			Caltech101			OxfordPets		
		Base	Novel	HM	Base	Novel	HM	Base	Novel	HM	Base	Novel	HM
CLIP	ICML22	69.34	74.22	71.70	72.43	68.14	70.22	96.84	94.00	95.40	91.17	97.26	94.12
CoOp	IJCV22	82.69	63.22	71.66	76.47	67.88	71.92	98.00	89.81	94.20	93.67	95.29	94.47
CoCoOp	CVPR22	80.47	71.69	75.83	77.60	70.75	74.00	97.96	93.81	95.84	95.20	97.69	96.43
MaPLe	CVPR23	82.28	75.14	78.55	76.66	70.54	73.47	97.74	94.36	96.02	95.43	97.76	96.58
PromptSRC	ICCV23	84.26	76.10	79.97	77.60	70.73	74.01	98.10	94.03	96.02	95.33	97.30	96.30
CoPrompt	ICLR24	84.00	77.23	80.48	77.67	71.27	74.33	98.27	94.90	96.55	95.87	98.10	96.87
TextRefiner	AAAI25	79.74	74.32	76.94	76.84	70.54	73.56	98.13	94.43	96.24	95.27	97.65	96.45
MMRL	CVPR25	85.68	77.16	81.20	77.90	71.30	74.45	98.97	94.50	96.68	95.90	97.60	96.74
ANprompt		86.15	77.70	81.70	77.83	71.17	74.35	98.97	94.73	96.80	95.73	97.17	96.44
Method	Ref.	StandfordCars			Flowers102			Food101			FGVCAircraft		
		Base	Novel	HM	Base	Novel	HM	Base	Novel	HM	Base	Novel	HM
CLIP	ICML22	63.37	74.89	68.65	72.08	77.80	74.83	90.10	91.22	90.66	27.19	36.29	31.09
CoOp	IJCV22	78.12	60.40	68.13	97.60	59.67	74.06	88.33	82.26	85.19	40.44	22.30	28.75
CoCoOp	CVPR22	70.49	73.59	72.01	94.87	71.75	81.71	90.70	91.29	90.99	33.41	23.71	27.74
MaPLe	CVPR23	72.94	74.00	73.47	95.92	72.46	82.56	90.71	92.05	91.38	37.44	35.61	36.50
PromptSRC	ICCV23	78.27	74.97	76.58	98.07	76.50	85.95	90.67	91.53	91.10	42.73	37.87	40.15
CoPrompt	ICLR24	76.97	74.40	75.66	97.27	76.60	85.71	90.73	92.07	91.40	40.20	39.33	39.76
TextRefiner	AAAI25	71.40	70.90	71.15	95.92	74.33	83.76	90.88	91.43	91.15	35.35	35.87	35.61
MMRL	CVPR25	81.30	75.07	78.06	98.97	77.27	86.78	90.57	91.50	91.03	46.30	37.03	41.15
ANprompt		83.57	74.63	78.85	98.60	77.30	86.66	90.63	91.50	91.06	49.67	36.60	42.14
Method	Ref.	SUN397			DTD			EuroSAT			UCF101		
		Base	Novel	HM	Base	Novel	HM	Base	Novel	HM	Base	Novel	HM
CLIP	ICML22	69.36	75.35	72.23	53.24	59.90	56.37	56.48	64.05	60.03	70.53	77.50	73.85
CoOp	IJCV22	80.60	65.89	72.51	79.44	41.18	54.24	92.19	54.74	68.69	84.69	56.05	67.46
CoCoOp	CVPR22	79.74	76.86	78.27	77.01	56.00	64.85	87.49	60.04	71.21	82.33	73.45	77.64
MaPLe	CVPR23	80.82	78.70	79.75	80.36	59.18	68.16	94.07	73.23	82.35	83.00	78.66	80.77
PromptSRC	ICCV23	82.67	78.47	80.52	83.37	62.97	71.75	92.90	73.90	82.30	87.10	78.80	82.74
CoPrompt	ICLR24	82.63	80.03	81.31	83.13	64.73	72.79	94.60	78.57	85.84	86.90	79.57	83.07
TextRefiner	AAAI25	80.96	76.49	78.66	75.35	58.09	65.60	74.57	75.82	73.68	82.52	75.01	78.59
MMRL	CVPR25	83.20	79.30	81.20	85.67	65.00	73.82	95.60	80.17	87.21	88.10	80.07	83.39
ANprompt		83.07	79.07	81.02	85.20	65.10	73.80	95.53	87.33	91.21	88.80	80.07	84.21

Cross-Dataset Evaluation Table 2 shows the performance comparison between our ANPrompt and existing methods in cross-dataset evaluation. On the ImageNet source dataset, ANPrompt shows comparable performance to other competitive methods. On the target domain dataset, ANPrompt achieved the best performance on six of the ten datasets, showing excellent generalization ability, especially on fine-grained datasets, such as FGVCAircraft and EuroSAT. Specifically, with an average of 10 datasets, ANPrompt achieved the highest accuracy rate of 67.14%. Meanwhile, compared with the suboptimal method CoPrompt, ANPrompt achieved 0.14% performance improvement. Different from the existing methods, we use the anti-noise visual prompt prototype to align the weak noise frozen text features to generate soft, context-aware supervision signals, thus improving cross-domain performance.

Domain Generalization We compare the performance of our ANPrompt with that of six previous methods on cross-

domain data sets. As shown in Table 3, the average performance of ANPrompt on four data sets exceeds that of most comparison methods, showing its strong cross-domain generalization ability. Specifically, ANPrompt performs best on Imagenet-V2 dataset, and it also shows considerable performance on other target domain datasets.

Ablation Experiments

Component Ablation We conduct an ablation study to evaluate the contribution of each component in ANPrompt, including the Weak noise Frozen Text feature (TextNoise), Weak Alignment Loss (WALoss), and Anti-noise Prompt injection. As shown in Table 4, introducing WALoss or Anti-Prompt individually yields consistent improvements over the baseline, with gains of +0.06 and +0.19 respectively. Notably, the addition of TextNoise leads to further gains when combined with either WALoss (+0.34) or Anti-Prompt (+0.40). When all three components are enabled, ANPrompt

Table 2: Results from cross-dataset evaluation. ANprompt provides the highest average accuracy.

	Source					Target							
	ImageNet	Caltech	Pets	Cars	Flowers	Food	Aircraft	SUN397	DTD	EuroSat	UCF101	Average	
CoOp	71.51	93.70	89.14	64.51	68.71	85.30	18.47	64.15	41.90	46.39	66.55	63.88	
CoCoOp	71.02	94.43	90.14	65.32	71.88	86.06	22.94	67.36	45.73	45.37	68.21	65.74	
MaPLe	70.72	93.53	90.55	65.57	72.23	86.20	24.74	67.01	46.49	48.06	68.06	66.10	
PromptSRC	71.27	93.60	90.25	65.70	70.25	86.15	23.90	67.10	46.87	45.50	68.75	65.81	
CoPrompt	70.80	94.50	90.75	65.67	72.70	86.43	20.40	67.57	47.07	51.90	69.73	67.00	
TAC	72.77	94.53	90.67	65.30	72.20	85.83	23.53	67.63	47.57	48.07	70.00	66.53	
ANprompt	71.13	94.70	91.00	66.00	72.87	86.23	26.10	67.47	45.83	51.97	69.27	67.14	

Table 3: Results on domain generalization task.

	Source		Target				Average
	ImageNet		-V2	-Sk	-A	-R	
CLIP	66.73	60.83	46.15	47.77	73.96	57.18	
CoOp	71.51	64.20	47.99	49.71	75.21	59.28	
CoCoOp	71.02	64.07	48.75	50.63	76.18	59.90	
MaPLe	70.72	64.07	49.15	50.90	76.98	60.26	
PromptSRC	71.27	64.35	49.55	50.90	77.80	60.63	
CoPrompt	70.80	64.25	49.43	50.50	77.51	60.42	
MMRL	72.03	64.47	49.17	51.20	77.53	60.59	
ANprompt	71.13	64.63	49.13	50.37	77.47	60.40	

achieves the highest harmonic mean (HM) of 81.70, surpassing the baseline by +0.79. These results verify the complementary nature of each module and their collective effectiveness in enhancing robustness under noise.

Table 4: The Effectiveness of different components in AN-Prompt. The TextNoise stands for the Weak noise Frozen Text feature.

TextNoise	WALoss	Anti-Prompt	HM
✗	✗	✗	80.91
✗	✓	✗	80.97(+0.06)
✗	✗	✓	81.10(+0.19)
✓	✓	✗	81.25(+0.34)
✗	✓	✓	81.27(+0.36)
✓	✗	✓	81.31(+0.40)
✓	✓	✓	81.70(+0.79)

Effect of Prompt Token Length. We study the effect of varying the number of prompt tokens T on performance. As shown in Table 5, increasing T from 1 to 5 gradually improves performance across base and novel classes, leading to a peak harmonic mean (HM) of 81.70% at $T = 5$. This suggests that moderate prompt length enhances generalization. However, performance saturates at $T = 6$, where no further gain is observed, which proved the effectiveness of the ablation experiment on token length. Therefore, setting

$T = 5$ offers the best trade-off between expressiveness and stability.

Table 5: The length of Prompt Token.

T	1	2	3	4	5	6
B	85.80	86.08	86.13	86.08	86.15	86.09
N	75.87	75.25	75.47	75.87	77.70	77.67
HM	80.53	80.30	80.45	80.66	81.70	81.66

Effect of weight of Weak Noise Frozen Text feature. We examine the sensitivity of ANPrompt to the weighting factor applied to the Weak Noise Frozen Text feature. As shown in Table 6, setting the weight to a small value (0.001) yields the best harmonic mean (81.70), indicating effective integration of weak noise signals. As the weight increases, performance on novel classes consistently degrades, leading to a gradual drop in HM. This trend suggests that overemphasizing the weak noise branch introduces distributional bias and harms generalization. These results highlight the necessity of a carefully balanced contribution from TextNoise.

Table 6: The Effectiveness of different weight of Weak Noise Frozen Text feature.

Weight	Base	Novel	HM
0.001	86.15	77.70	81.70
0.01	86.10	76.84	81.21
0.1	86.09	76.48	81.00
1.0	86.02	75.51	80.43

Conclusion

We proposed ANPrompt, a robust prompt tuning framework that explicitly models weak semantic perturbations to improve generalization in vision-language models. By injecting weak semantic perturbation into the alignment process and prompt representation, ANPrompt enhances robustness under the weak semantic perturbation. Experimental results on 11 benchmarks demonstrate its clear advantages over existing methods, highlighting the effectiveness of incorporating weak semantic perturbation noise into prompt tuning.

Acknowledgments

This work is supported by the National Natural Science Foundation of China (62376106).

References

Bossard, L.; Guillaumin, M.; and Gool, L. V. 2014. Food-101 - Mining Discriminative Components with Random Forests. In *European Conference on Computer Vision*, 446–461.

Chen, Y.; Qiao, X.; Sun, Z.; and Li, X. 2024. ComKD-CLIP: Comprehensive Knowledge Distillation for Contrastive Language-Image Pre-training Model. *arXiv preprint arXiv:2408.04145*.

Cimpoi, M.; Maji, S.; Kokkinos, I.; Mohamed, S.; and Vedaldi, A. 2014. Describing textures in the wild. In *Computer Vision and Pattern Recognition*, 3606–3613.

Deng, J.; Dong, W.; Socher, R.; Li, L.-J.; Li, K.; and Fei-Fei, L. 2009. Imagenet: A large-scale hierarchical image database. In *Computer Vision and Pattern Recognition*, 248–255.

Farina, M.; Mancini, M.; Iacca, G.; and Ricci, E. 2025. Rethinking Few-Shot Adaptation of Vision-Language Models in Two Stages. *arXiv preprint arXiv:2503.11609*.

Fei-Fei, L.; Fergus, R.; and Perona, P. 2004. Learning generative visual models from few training examples: An incremental bayesian approach tested on 101 object categories. In *Computer Vision and Pattern Recognition workshop*, 178–178.

Feng, C.; Tzimiropoulos, G.; and Patras, I. 2024. Clip-cleaner: Cleaning noisy labels with clip. In *Proceedings of the 32nd ACM International Conference on Multimedia*, 876–885.

Gao, P.; Geng, S.; Zhang, R.; Ma, T.; Fang, R.; Zhang, Y.; Li, H.; and Qiao, Y. 2024. Clip-adapter: Better vision-language models with feature adapters. *International Journal of Computer Vision*, 132(2): 581–595.

Guo, Y.; and Gu, X. 2024. JoAPR: Cleaning the Lens of Prompt Learning for Vision-Language Models. In *Proceedings of the IEEE/CVF Conference on Computer Vision and Pattern Recognition*, 28695–28705.

Guo, Y.; and Gu, X. 2025. Mmrl: Multi-modal representation learning for vision-language models. In *Proceedings of the Computer Vision and Pattern Recognition Conference*, 25015–25025.

Hao, F.; He, F.; Wu, F.; Wang, T.; Song, C.; and Cheng, J. 2025. Task-Aware Clustering for Prompting Vision-Language Models. In *Proceedings of the Computer Vision and Pattern Recognition Conference*, 14745–14755.

Helber, P.; Bischke, B.; Dengel, A.; and Borth, D. 2019. Euruosat: A novel dataset and deep learning benchmark for land use and land cover classification. *IEEE Journal of Selected Topics in Applied Earth Observations and Remote Sensing*, 12(7): 2217–2226.

Hendrycks, D.; Basart, S.; Mu, N.; Kadavath, S.; Wang, F.; Dorundo, E.; Desai, R.; Zhu, T.; Parajuli, S.; Guo, M.; et al. 2021a. The Many Faces of Robustness: A Critical Analysis of Out-of-Distribution Generalization. In *International Conference on Computer Vision*, 8340–8349.

Hendrycks, D.; Zhao, K.; Basart, S.; Steinhardt, J.; and Song, D. 2021b. Natural Adversarial Examples. In *Computer Vision and Pattern Recognition*, 15262–15271.

Hua, C.; Xu, Q.; Yang, Z.; Wang, Z.; Bao, S.; and Huang, Q. 2025. OpenworldAUC: Towards Unified Evaluation and Optimization for Open-world Prompt Tuning. *arXiv preprint arXiv:2505.05180*.

Huang, R.; Long, Y.; Han, J.; Xu, H.; Liang, X.; Xu, C.; and Liang, X. 2023. Nlip: Noise-robust language-image pre-training. In *Proceedings of the AAAI Conference on Artificial Intelligence*, volume 37, 926–934.

Jia, C.; Yang, Y.; Xia, Y.; Chen, Y.-T.; Parekh, Z.; Pham, H.; Le, Q.; Sung, Y.-H.; Li, Z.; and Duerig, T. 2021. Scaling up visual and vision-language representation learning with noisy text supervision. In *International conference on machine learning*, 4904–4916. PMLR.

Kay, W.; Carreira, J.; Simonyan, K.; Zhang, B.; Hillier, C.; Vijayanarasimhan, S.; Viola, F.; Green, T.; Back, T.; Natsev, P.; et al. 2017. UCF101: A dataset of 101 human actions classes from videos in the wild. In *arXiv preprint arXiv:1212.0402*.

Khattak, M. U.; Naeem, M. F.; Naseer, M.; Van Gool, L.; and Tombari, F. 2024. Learning to prompt with text only supervision for vision-language models. *arXiv preprint arXiv:2401.02418*.

Khattak, M. U.; Rasheed, H.; Maaz, M.; Khan, S.; and Khan, F. S. 2023a. Maple: Multi-modal prompt learning. In *Computer Vision and Pattern Recognition*, 19113–19122.

Khattak, M. U.; Wasim, S. T.; Naseer, M.; Khan, S.; Yang, M.-H.; and Khan, F. S. 2023b. Self-regulating prompts: Foundational model adaptation without forgetting. In *Proceedings of the IEEE/CVF international conference on computer vision*, 15190–15200.

Krause, J.; Stark, M.; Deng, J.; and Fei-Fei, L. 2013. 3d object representations for fine-grained categorization. In *International Conference on Computer Vision workshops*, 554–561.

Lafon, M.; Ramzi, E.; Rambour, C.; Audebert, N.; and Thome, N. 2024. Gallop: Learning global and local prompts for vision-language models. In *European Conference on Computer Vision*, 264–282. Springer.

Li, H.; Cao, H.; Feng, B.; Shao, Y.; Tang, X.; Yan, Z.; Yuan, L.; Tian, Y.; and Li, Y. 2025a. Beyond Chemical QA: Evaluating LLM’s Chemical Reasoning with Modular Chemical Operations. *arXiv preprint arXiv:2505.21318*.

Li, H.; Huang, J.; Jin, P.; Song, G.; Wu, Q.; and Chen, J. 2023. Weakly-supervised 3d spatial reasoning for text-based visual question answering. *IEEE Transactions on Image Processing*, 32: 3367–3382.

Li, H.; Jia, Y.; Jin, P.; Cheng, Z.; Li, K.; Sui, J.; Liu, C.; and Yuan, L. 2024a. Freestyleret: retrieving images from style-diversified queries. In *European Conference on Computer Vision*, 258–274. Springer.

Li, H.; Wang, L.; Wang, C.; Jiang, J.; Peng, Y.; and Long, G. 2025b. Dpc: Dual-prompt collaboration for tuning vision-language models. In *Proceedings of the Computer Vision and Pattern Recognition Conference*, 25623–25632.

Li, J.; Li, D.; Xiong, C.; and Hoi, S. 2022. Blip: Bootstrapping language-image pre-training for unified vision-language understanding and generation. In *International conference on machine learning*, 12888–12900. PMLR.

Li, Z.; Li, X.; Fu, X.; Zhang, X.; Wang, W.; Chen, S.; and Yang, J. 2024b. Promptkd: Unsupervised prompt distillation for vision-language models. In *Proceedings of the IEEE/CVF Conference on Computer Vision and Pattern Recognition*, 26617–26626.

Li, Z.; Song, Y.; Cheng, M.-M.; Li, X.; and Yang, J. 2024c. Advancing Textual Prompt Learning with Anchored Attributes. *arXiv preprint arXiv:2412.09442*.

Maji, S.; Rahtu, E.; Kannala, J.; Blaschko, M.; and Vedaldi, A. 2013. Fine-grained visual classification of aircraft. In *arXiv preprint arXiv:1306.5151*.

Nilsback, M.-E.; and Zisserman, A. 2008. Automated flower classification over a large number of classes. In *Sixth Indian Conference on Computer Vision*, 722–729.

Pan, B.; Li, Q.; Tang, X.; Huang, W.; Fang, Z.; Liu, F.; Wang, J.; Yu, J.; and Shi, Y. 2025. NLPrompt: Noise-Label Prompt Learning for Vision-Language Models. In *Proceedings of the Computer Vision and Pattern Recognition Conference*, 19963–19973.

Parkhi, O. M.; Vedaldi, A.; Zisserman, A.; and Jawahar, C. 2012. Cats and dogs. In *Computer Vision and Pattern Recognition*, 3498–3505.

Radford, A.; Kim, J. W.; Hallacy, C.; Ramesh, A.; Goh, G.; Agarwal, S.; Sastry, G.; Askell, A.; Mishkin, P.; Clark, J.; et al. 2021. Learning transferable visual models from natural language supervision. In *International Conference on Machine Learning*, 8748–8763.

Recht, B.; Roelofs, R.; Schmidt, L.; and Shankar, V. 2019. Do ImageNet Classifiers Generalize to ImageNet? In *International Conference on Machine Learning*, 5389–5400.

Roy, S.; and Etemad, A. 2024. Consistency-guided Prompt Learning for Vision-Language Models. In *International Conference on Learning Representations*.

Shi, B.; Xu, Z.; Jia, S.; and Ma, C. 2024. Prompt learning with quaternion networks. In *The Twelfth International Conference on Learning Representations*.

Song, L.; Xue, R.; Wang, H.; Sun, H.; Ge, Y.; Shan, Y.; et al. 2023. Meta-adapter: An online few-shot learner for vision-language model. *Advances in Neural Information Processing Systems*, 36: 55361–55374.

Tian, X.; Zou, S.; Yang, Z.; and Zhang, J. 2024. Argue: Attribute-guided prompt tuning for vision-language models. In *Proceedings of the IEEE/CVF Conference on Computer Vision and Pattern Recognition*, 28578–28587.

Wang, H.; Ge, S.; Lipton, Z.; and Xing, E. P. 2019. Learning Robust Global Representations by Penalizing Local Predictive Power. *Neural Information Processing Systems*, 32: 1–13.

Wang, Y.; Jiang, X.; Cheng, D.; Li, D.; and Zhao, C. 2024. Learning hierarchical prompt with structured linguistic knowledge for vision-language models. In *Proceedings of the AAAI conference on artificial intelligence*, volume 38, 5749–5757.

Weng, Z.; Yang, X.; Li, A.; Wu, Z.; and Jiang, Y.-G. 2023. Open-vclip: Transforming clip to an open-vocabulary video model via interpolated weight optimization. In *International conference on machine learning*, 36978–36989. PMLR.

Wu, G.; Zhang, X.; Li, Z.; Chen, Z.; Liang, J.; Yang, J.; and Li, X. 2024. Cascade prompt learning for vision-language model adaptation. In *European Conference on Computer Vision*, 304–321. Springer.

Xiao, J.; Hays, J.; Ehinger, K. A.; Oliva, A.; and Torralba, A. 2010. Sun database: Large-scale scene recognition from abbey to zoo. In *Computer Vision and Pattern Recognition*, 3485–3492.

Xie, J.; Zhang, Y.; Peng, J.; Huang, Z.; and Cao, L. 2025. TextRefiner: Internal Visual Feature as Efficient Refiner for Vision-Language Models Prompt Tuning. In *Proceedings of the AAAI Conference on Artificial Intelligence*, volume 39, 8718–8726.

Xu, G.; Jin, P.; Wu, Z.; Li, H.; Song, Y.; Sun, L.; and Yuan, L. 2024. Llava-cot: Let vision language models reason step-by-step. *arXiv preprint arXiv:2411.10440*.

Yang, C.; An, Z.; Huang, L.; Bi, J.; Yu, X.; Yang, H.; Diao, B.; and Xu, Y. 2024a. Clip-kd: An empirical study of clip model distillation. In *Proceedings of the IEEE/CVF Conference on Computer Vision and Pattern Recognition*, 15952–15962.

Yang, L.; Zhang, R.-Y.; Wang, Y.; and Xie, X. 2024b. Mma: Multi-modal adapter for vision-language models. In *Proceedings of the IEEE/CVF Conference on Computer Vision and Pattern Recognition*, 23826–23837.

Yao, H.; Zhang, R.; and Xu, C. 2024. Tcp: Textual-based class-aware prompt tuning for visual-language model. In *Proceedings of the IEEE/CVF Conference on Computer Vision and Pattern Recognition*, 23438–23448.

Yao, L.; Huang, R.; Hou, L.; Lu, G.; Niu, M.; Xu, H.; Liang, X.; Li, Z.; Jiang, X.; and Xu, C. 2021. Filip: Fine-grained interactive language-image pre-training. *arXiv preprint arXiv:2111.07783*.

Yuan, L.; Chen, D.; Chen, Y.; Codella, N.; Dai, X.; Gao, J.; Hu, H.; Huang, X.; Li, B.; Li, C.; et al. 2021. Florence: A new foundation model for computer vision. *arXiv 2021. arXiv preprint arXiv:2111.11432*.

Zhai, X.; Wang, X.; Mustafa, B.; Steiner, A.; Keysers, D.; Kolesnikov, A.; and Beyer, L. 2022. Lit: Zero-shot transfer with locked-image text tuning. In *Proceedings of the IEEE/CVF conference on computer vision and pattern recognition*, 18123–18133.

Zhang, J.; Wu, S.; Gao, L.; Shen, H. T.; and Song, J. 2024. Dept: Decoupled prompt tuning. In *Proceedings of the IEEE/CVF Conference on Computer Vision and Pattern Recognition*, 12924–12933.

Zhou, K.; Yang, J.; Loy, C. C.; and Liu, Z. 2022a. Conditional prompt learning for vision-language models. In *Computer Vision and Pattern Recognition*, 16795–16804.

Zhou, K.; Yang, J.; Loy, C. C.; and Liu, Z. 2022b. Learning to prompt for vision-language models. In *International Journal of Computer Vision*, 2337–2348.

Zhu, B.; Niu, Y.; Han, Y.; Wu, Y.; and Zhang, H. 2023. Prompt-aligned gradient for prompt tuning. In *Proceedings of the IEEE/CVF international conference on computer vision*, 15659–15669.

Zhu, Y.; Ji, Y.; Zhao, Z.; Wu, G.; and Wang, L. 2024. Awt: Transferring vision-language models via augmentation, weighting, and transportation. *Advances in Neural Information Processing Systems*, 37: 25561–25591.